

BEAM TOMOGRAPHY IN TWO AND FOUR DIMENSIONS\*

O. R. Sander, G. N. Minerbo, R. A. Jameson,  
and D. D. Chamberlin  
Los Alamos Scientific Laboratory  
Los Alamos, New Mexico 87545

Summary

The coming generations of high beam-power accelerators require new techniques to monitor the emittance and the shape of the beam; in particular, measurements that do not interfere with the beam itself are necessary. A new computational algorithm, MENT (Maximum ENTropy), will be presented that combines nondestructive profile measurements taken from a number of stations along the beam line, with beam-dynamics calculations to compute a four-dimensional phase-space distribution. A version of MENT has been used on experimental data to reconstruct the two-dimensional transverse emittance of the Clinton P. Anderson Meson Physics Facility (LAMPF) proton beam at 100 MeV and the  $H^-$  beam at 750 KeV. Wire scanners at three stations were used to get the one-dimensional profiles. Results will be compared with those gained using the destructive slit and collector method and with those gained using MART (Multiplicative Algebraic Reconstruction Technique) on the same three profiles.

Maximum Entropy Reconstruction Techniques

Two algorithms were used, MART<sup>1</sup> (Multiplicative Algebraic Reconstruction Technique), and MENT,<sup>2</sup> to reconstruct the emittance of LAMPF beams at 100-MeV and 750-KeV energies. Both algorithms were used to reconstruct a source from the same sets of projections or profiles. Both MENT and MART are designed to converge to a maximum entropy solution, or yield an image with the lowest information content consistent with available data; extraneous information or artificial structure is thereby avoided. Because a description of MENT and MART for two dimensional reconstruction has been given elsewhere,<sup>1,2</sup> only comments on these methods will be given. Theoretically both algorithms, when applied to distributions of Gaussian shape, should produce essentially exact reconstruction. MART and MENT are well suited for applications where the number of measured profiles is small and where the source distribution is somewhat Gaussian in shape. These attributes made the algorithms attractive for accelerator application because particle-beam distributions are usually smooth, unimodal, possess only moderate amounts of asymmetry and are often available for measurement at only a few stations. MENT has been used for cross-section reconstruction of

fuel rod-bundles<sup>3</sup> and laser-imploded pellets.<sup>4</sup> MART has been used to reconstruct transverse emittances of particle beams.<sup>5</sup> In principle, MENT is simpler to implement because it only requires the use of one-dimensional measured profiles and one-dimensional back projections; MART requires not only the same one-dimensional measured profiles but also an array representation of the source. The array size can become considerable as one goes to three, four, or n dimensions. The amount of computer storage for the array is  $M^n$ , where M is the number of samples in a projection and typically varies between 50 and 100. This storage requirement eliminates the use of small and medium-size computers. The array must be transferred from one station to another by a complicated mapping of the  $M^n$  pixel-volume elements. This mapping has not been attempted for any n greater than two, and appears quite formidable for any greater n. However, the extension of MENT to four or six dimensions is straightforward. For these reasons, MENT was adopted to reconstruct transverse emittance distributions and its performance investigated in comparison to MART.

Method

Three wire scanners in the 100-MeV and in the 750-KeV transport regions of LAMPF were used to measure the beam profiles. The wire scanners were separated by nearly equal drift sections located near standard emittance measuring stations consisting of slits and collectors. At 100 MeV, the  $H^+$  beam transmitted through the slit was observed on a wire scanner. These data were reported earlier.<sup>5</sup> When compared to the data collected with the standard slit method, the MART reconstruction had small differences in the ellipse parameters  $\alpha$  and  $\beta$ , which could not be attributed to statistics. In the comparison of the emittance area versus percentage of total beam enclosed, both MART and the standard method results were in excellent agreement. These same profiles now have been analyzed with the MENT algorithm.

Similar measurements were made of the LAMPF low-intensity  $H^-$  beam at 750 KeV. In this case the standard emittance station used a collector consisting of a plate with conducting strips attached to it. At both energies, it was assumed that no space-charge effects were present and that the transfer matrices connecting the viewing stations were simple drifts, which they are in the zero current limit.

\*Work performed under the auspices of the U. S. Department of Energy.

**Results**

Figures 1 and 2 show plots of emittance area versus percentage of total beam for beams of 100-MeV and 750-KeV energy. In both cases, MENT and MART are in good agreement with the data gained with the slit and collector method, which is assumed to yield a density distribution closest to the true beam distribution.

The shape parameters  $\alpha$  and  $\beta$  have been compared by displaying the residual betatron oscillation  $\Delta R/R$  for MENT and MART. The true ellipse parameters are assumed equal to those gained with the slit and collector method. In Fig. 3  $\Delta R/R$  for the 750-KeV data is shown. Both algorithms give excellent reconstructions of the emittance distribution. Similar plots for the 100-MeV data are also shown in Fig. 3. Both methods give values of  $\Delta R/R$  approximately equal to 0.1. In this case the MENT results more closely match the slit and collector results. Contour plots of the reconstructed density distribution are shown in Fig. 4 for the slit and collector method, in Fig. 5 for the MART algorithm and in Fig. 6 for the MENT algorithm.

Because situations could exist where the matching of a beam emittance to a linac acceptance should result in a value of  $\Delta R/R$  as small as 0.1, an emittance-measuring method whose accuracy can be characterized by a value of  $\Delta R/R$  smaller than 0.1 is desired. Therefore, corrections that will reduce the value of  $\Delta R/R$  in Fig. 3 are sought. It has been determined that this small but significant value cannot be attributed to errors caused by non-ideal viewing

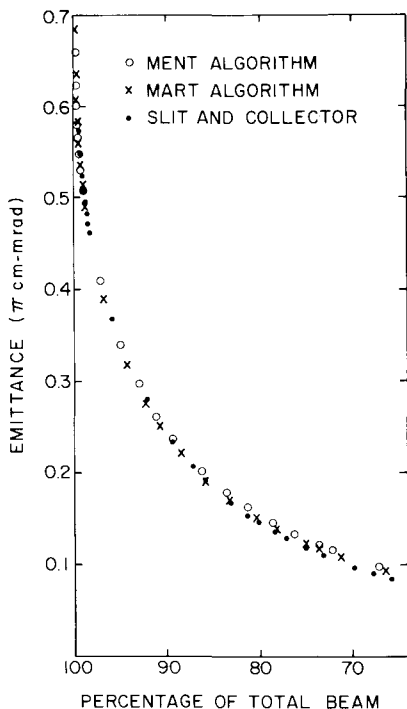


Fig. 1. Total emittances versus percentage of the 100-MeV  $H^+$  beam.

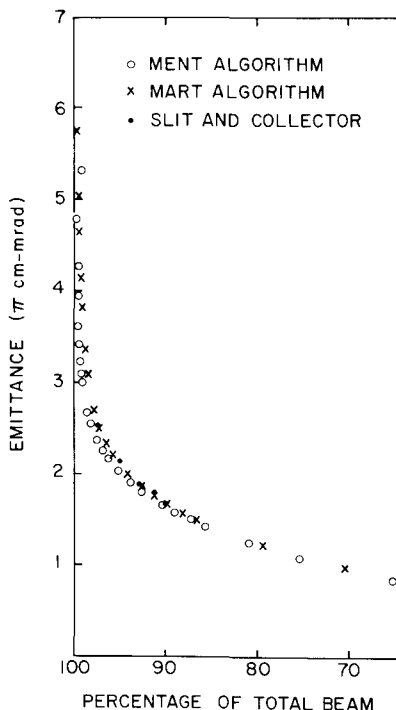


Fig. 2. Total emittance versus percentage of the 750-keV  $H^-$  beam.

angles or any artificial asymmetric emittance growth caused by the pixel mapping in MART.

An additional test of the algorithms was made using generated asymmetric Gaussian distributions. Both MART and MENT gave nearly exact reconstructions. In this case our version of MART is superior to earlier versions that gave reconstructions with jagged peaks and fluctuations. The improvement is apparently the result of reconstructing profiles from column sums of transformed pixels. Profiles were previously calculated from rays intercepting pixels.

Four-Dimensional Reconstruction Method

The MENT algorithm was chosen to reconstruct four-dimensional emittance distributions because it gives equally good, or slightly better, two-dimensional reconstruction and because it is relatively easy to expand MENT to four dimensions. For the present reconstruction only in linac sections where no energy change takes place, where first-order optics is valid, and where space-charge effects can be expressed by a linear transfer matrix, will be considered.

The phase-space density function of the beam in a reference plane  $z = 0$  can be denoted by

$$f \left( \begin{bmatrix} x \\ x' \\ y \\ y' \end{bmatrix} \right), \tag{1}$$

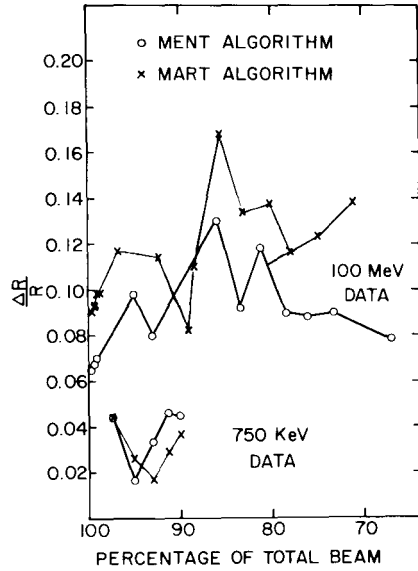


Fig. 3. Comparison of the reconstructed ellipses.

where  $x$  and  $y$  are the coordinates of the particle, and where the direction unit vector  $\Omega = p/p$ , ( $p$  is the particle momentum) has components  $x', y'$ . At station  $j$  (in the plane  $z = z_j$ ) the particle will have coordinates given by:

$$\begin{pmatrix} x_j \\ x'_j \\ y_j \\ y'_j \end{pmatrix} = T_j \begin{pmatrix} x \\ x' \\ y \\ y' \end{pmatrix}, \quad (2)$$

where  $T_j$  is a  $4 \times 4$  transfer matrix. Computer codes, e.g., TRACE<sup>7</sup> and TRANSPORT,<sup>8</sup> are available to compute transfer matrices for different accelerator components. The density distribution at plane  $z = z_j$  is, from Eqs. (1) and (2),

$$f \left( \begin{bmatrix} x_j \\ x'_j \\ y_j \\ y'_j \end{bmatrix} \right) = f \left( T_j^{-1} \begin{bmatrix} x \\ x' \\ y \\ y' \end{bmatrix} \right). \quad (3)$$

Consider now a scan measurement at station  $j$  that produces a projection of the beam density along a line making an angle  $\theta_k$  with the positive  $x$ -axis. These one-dimensional profiles can be obtained, for example, with the wire scanner technique, or by observing light quanta emitted by suitable tracer materials or

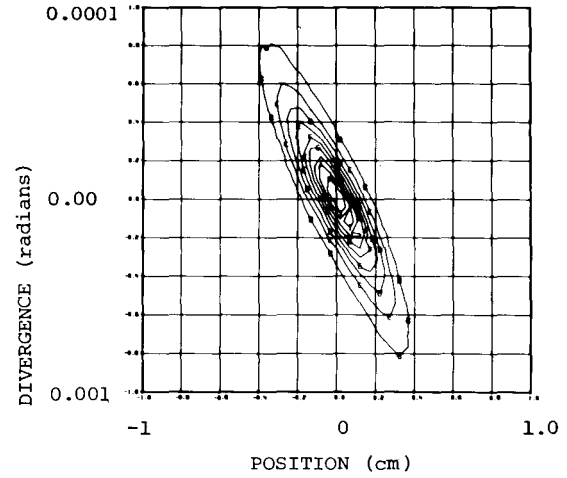


Fig. 4. Beam contours from the slit and collector method.

background gas ionization. To express the measured profile in terms of  $f$ , introduce a matrix  $R$  that produces a rotation of axes through an angle  $\theta_k$  about the  $z$ -axis:

$$\begin{pmatrix} u_{kj} \\ u'_{kj} \\ v_{kj} \\ v'_{kj} \end{pmatrix} = R(\theta_k) \begin{pmatrix} x_j \\ x'_j \\ y_j \\ y'_j \end{pmatrix}, \quad (4)$$

where

$$R(\theta) = \begin{pmatrix} \cos\theta & 0 & \sin\theta & 0 \\ 0 & \cos\theta & 0 & \sin\theta \\ -\sin\theta & 0 & \cos\theta & 0 \\ 0 & -\sin\theta & 0 & \cos\theta \end{pmatrix}. \quad (5)$$

The measured projection profile for the angle  $\theta_k$  at station  $z_j$  is;

$$g_{kj}(u) = \int dv \int du' \int dv' f \left( T_j^{-1} R_k^{-1} \begin{bmatrix} u \\ u' \\ v \\ v' \end{bmatrix} \right) \quad (6)$$

$j = 1, \dots, J, \quad k = 1, \dots, K$

Now consider the entropy associated with the distribution  $f$ . Assume that  $f$  satisfies the conditions:

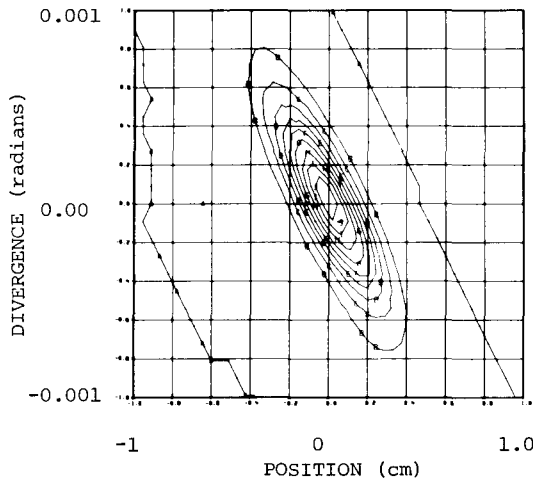


Fig. 5. Beam contours from the MART algorithm.

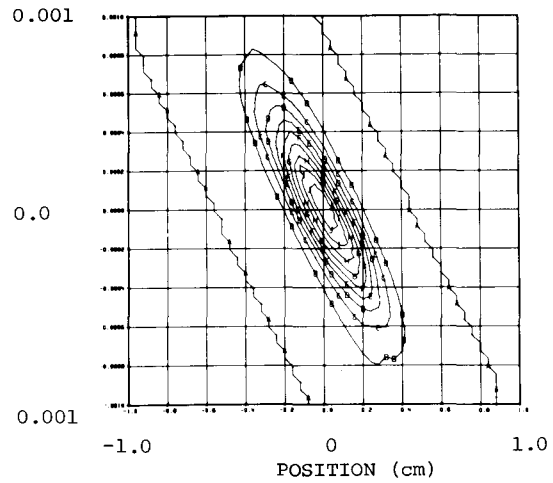


Fig. 6. Beam contours from the MENT algorithm.

$$f \left( \begin{bmatrix} x \\ x' \\ y \\ y' \end{bmatrix} \right) \geq 0 \quad (7)$$

$$\int dx \int dx' \int dy \int dy' f \left( \begin{bmatrix} x \\ x' \\ y \\ y' \end{bmatrix} \right) = 1,$$

so that  $f$  can be regarded as a probability distribution function. These conditions imply that:

$$g_{kj}(u) \geq 0 \quad j = 1, \dots, J \quad k = 1, \dots, K, \\ \int du g_{kj}(u) = 1. \quad (8)$$

The entropy associated with  $f$  is:<sup>1</sup>

$$H = - \int_D dx \int dx' \int dy \int dy' f \left( \begin{bmatrix} x \\ x' \\ y \\ y' \end{bmatrix} \right) \ln \left\{ f \left( \begin{bmatrix} x \\ x' \\ y \\ y' \end{bmatrix} \right) V \right\}, \quad (9)$$

where  $V$  is the 4-dimensional volume of the set  $D$  where  $f$  is positive. Now maximize  $H$  with Eqs. (6) treated as constraints. This prescription produces the solution that is the "most probable" consistent with the measured data for  $g$ . The Lagrange multiplier method is used to solve this optimization problem.

Introduce a Lagrange multiplier  $\lambda_{kj}(u)$ , for each condition in Eq. (6) and perform a variation of the functional:

$$\eta(f) = H - \sum_{kj} \int du \lambda_{kj}(u) \left\{ g_{kj}(u) - \int dx \int dx' \int dy \int dy' \cdot f \left( T_j^{-1} R_k^{-1} \begin{bmatrix} u \\ u' \\ v \\ v' \end{bmatrix} \right) \right\}. \quad (10)$$

By changing variables of integration the second integral in Eq. (10) can be rewritten as;

$$\sum_{kj} \int dx \int dx' \int dy \int dy' \lambda_{kj} \left( S_k T_j \begin{bmatrix} x \\ x' \\ y \\ y' \end{bmatrix} \right) f \left( \begin{bmatrix} x \\ x' \\ y \\ y' \end{bmatrix} \right), \quad (11)$$

where  $S_k$  is a  $1 \times 4$  submatrix of the matrix  $R_k$ :

$$S_k = [ \cos\theta_n \quad 0 \quad \sin\theta_n \quad 0 ] \quad (12)$$

The functional derivative of  $\eta$  with respect to  $f$  is set equal to zero, giving:

$$-\ln \{ f(\zeta) V \} - 1 + \sum_{kj} \lambda_{kj} (S_k T_j \zeta) = 0. \quad (13)$$

Thus  $f$  must have the form:

$$f(\zeta) = \frac{1}{V} \prod_{kj} h_{kj} (S_k T_j \zeta), \quad (14)$$

where

$$h_{jk}(u) = \exp \left[ \lambda_{kj}(u) - \frac{1}{KJ} \right] . \quad (15)$$

To find the unknown functions  $h_{kj}$ , solve the KJ equations obtained by substituting Eq. (14) into the constraint equations (6):

$$g_{kj}(u) = \frac{1}{V} h_{kj}(u) \int du' \int dv \int dv' \prod_{m, \ell \neq k, j} h_{m\ell} \cdot \left( S_m^T T_\ell^{-1} R_j^{-1} R_k^{-1} \begin{bmatrix} u \\ u' \\ v \\ v' \end{bmatrix} \right) . \quad (16)$$

The iteration scheme described in Ref. 1 must be modified as follows. Initially one sets

$$h_{kj}^0(u) = \begin{cases} 1 & \text{if } g_{kj}(u) \neq 0 \\ 0 & \text{if } g_{kj}(u) = 0 \end{cases} , \quad (17)$$

and one then applies cyclic updates:

$$h_{kj}^{i+1}(u) = h_{kj}^i / R_j^i(u),$$

if  $g_{kj}(u) \neq 0$  and  $k + (j-1)K = \text{imod}(JK) + 1$

$$h_{kj}^{i+1} = h_{kj}^i(u) \text{ otherwise,} \quad (18)$$

where

$$R_{kj}^i(u) = [g_{kj}(u)V]^{-1} h_{kj}^i(u) \int du' \int dv \int dv' \prod_{m, \ell \neq k, j} h_{m\ell}^i \left( S_m^T T_\ell^{-1} R_j^{-1} R_k^{-1} \begin{bmatrix} u \\ u' \\ v \\ v' \end{bmatrix} \right) . \quad (19)$$

This iteration scheme has been found to converge very fast numerically in two and three dimensions.

### Future Studies

We plan to use MENT to reconstruct emittance distributions for the Hanford FMIT Accelerator where the 3.5-MW beam power precludes standard interceptive sensors. Light emitted from ionized or excited residual gases in the beam region will be collected by low-level TV cameras and digitized. Beam profiles from four views at each of three stations will be used to reconstruct the 4-dimensional distribution.

At LAMPF we are adding additional wires at our 750-KeV wire scanner stations. These wires will give us additional views with which to reconstruct the 4-dimensional emittance. We are also conducting studies to determine how space-charge effects must be incorporated into our transfer matrices connecting viewing stations, and we plan to develop a method for assigning coordinates from the reconstructed distribution to a macroparticle distribution for use in computer simulation codes.

### References

1. J. S. Fraser, "Beam Tomography or ART in Accelerator Physics," Los Alamos Scientific Laboratory report LA-7498-MS (Nov. 1978).
2. G. Minerbo, "MENT: A Maximum Entropy Algorithm for Reconstructing a Source from Projection Data," Computer Graphics and Image Processing 10, 48 (1979).
3. T. G. Sanderson, "Reconstruction of Fuel Pin Bundles by a Maximum Entropy Method," IEEE Transactions on Nuclear Science, Vol. NS 26, 2685 (1979).
4. D. B. van Hulsteyn, P. Lee, J. G. Sanderson, G. N. Minerbo, "Three-Dimensional Reconstruction of X-Ray Emission in Laser Imploded Targets," Los Alamos Scientific Laboratory report LA-UR-78-3033, to be published in Applied Optics.
5. O. R. Sander, R. A. Jameson, R. D. Patton, "Recent Improvements in Beam Diagnostic Equipment," IEEE Transaction on Nuclear Science, Vol. NS 26, 3417 (1979).
6. J. Guyard, M. Weiss, "Use of Beam Emittance Measurements in Matching Problems," Proc. 19th Proton Linear Accelerator Conference, Chalk River, Canada, AECA 5677, Nov. 1974.
7. K. R. Crandall, "TRACE - An Interactive Beam Transport Program," Los Alamos Scientific Laboratory Report LA-5532, Oct. 1973.
8. K. L. Brown, B. K. Lear and S. K. Howry, "TRANSPORT/360," Stanford Linear Accelerator Center Report SLAC-91, 1977.